Nonlinear Regge trajectories and saturation of the Hagedorn spectrum

István Szanyi,[1,2,3,*] Tamás Biró,[1,†] László Jenkovszky,[4,‡] and Vladyslav Libov[4,§]
[1]*Wigner Research Centre for Physics, P. O. Box 49, H-1525 Budapest 114, Hungary*
[2]*Eötvös University, Pázmány Péter sétány (P.s.) 1/A, H-1117 Budapest, Hungary*
[3]*MATE Institute of Technology, Károly Róbert Campus, Mátrai út 36, H-3200 Gyöngyös, Hungary*
[4]*Bogolyubov Institute for Theoretical Physics (BITP), Ukrainian National Academy of Sciences 14-b, Metrologicheskaya Street, Kiev 03680, Ukraine*

(Received 28 August 2022; revised 18 November 2022; accepted 21 December 2022; published 6 February 2023)

We argue that two seemingly different phenomena, namely the well-known saturation of the Hagedorn exponential distribution and the less familiar saturation of Regge trajectories at resonance masses $m \approx 2$–2.5 GeV, are related and have the same origin: quark deconfinement. We show that the slope of the real part of nonlinear Regge trajectories determines the prefactor $f(m)$ in Hagedorn's resonance mass density distribution $\rho(m)$. While the Hagedorn distribution comes from statistics, Regge trajectories contain dynamics.

DOI: 10.1103/PhysRevC.107.024904

I. INTRODUCTION

The spectrum of hadron resonances is among the central problems of high-energy physics. The properties of highly excited resonances are intimately connected with the problem of confinement. We revise the spectrum of hadronic resonances by relating seemingly two different viewpoints: statistical (Hagedorn) and dynamical (Regge).

The density of hadron states follows the law [1]

$$\rho(m) = f(m)\exp(m/T_H), \tag{1}$$

where $f(m)$ is a slowly varying function of mass and T_H is the Hagedorn temperature, originally considered as the limiting temperature but later interpreted as the temperature of the color deconfinement phase transition where hadrons "boil," transforming the matter into a boiling quark-gluon soup.

Over 50 years after the publication of Hagedorn's paper [1] on the spectrum of resonances, many important details still remain open. In spite of many efforts by different groups of authors [2–5] involving more new data on resonances, the calculated value of the Hagedorn temperature shows a surprisingly wide spread from $T_H = 141$ MeV to $T_H = 340$ MeV, depending on the parametrization and the set of data (baryons, mesons) used. The discrepancies may have different origins, in particular (a) the large uncertainties in the specification and identification of heavy resonances and (b) the analytical form of the Hagedorn spectrum, in particular, the form of the function $f(m)$ multiplying Hagedorn's exponential. In the present paper, we address both issues.

In our analyses, we rely on the latest results of the Particle Data Group [6]. At the same time, we are aware of recent important developments and progress in theoretical studies of the Hagedorn spectrum and of the ultimate temperature based on gauge theories [7], lattice quantum chromodynamics (QCD) (by which one distinguishes between two different types of resonances: isolated ones in vacuum and resonance at a certain temperature), strings, and supergravity [8–10]. Its possible manifestation in the early universe was discussed in Refs. [11–13].

Our approach, however, is limited to the world of observed resonances, summarized by the Particle Data Group, and theoretical methods based on analyticity, unitarity, and duality.

Crucial and original in our paper is the identification of the function $f(m)$ with the derivative of the relevant Regge trajectory. In the spirit of the analytic S-matrix approach, Regge trajectories encode an essential part of the strong interaction dynamics; they are building blocks of the theory. There were many attempts to find analytic forms of the nonlinear complex Regge trajectories, based on mechanical analogs (string), quantum chromodynamics, etc., suggesting different and approximate solutions applicable in a limited range. In our approach, we rely on duality and constraints based on analyticity and unitarity, constraining the threshold and asymptotic behavior of the trajectories. An important constraint affecting the spectrum near its critical point is an upper bound on the real part of Regge trajectories, coming from dual models with Mandelstam analyticity [14]. Construction of explicit models of the trajectories satisfying the above constraints is a nontrivial problem. In the present paper, we propose explicit models of such trajectories allowing explicit calculations and compatible with the data on resonances.

Below we argue that while Hagedorn's exponential rise comes mainly from the proliferation of spin and isospin

*szanyi.istvan@wigner.hu
†biro.tamas@wigner.hu
‡jenk@bitp.kiev.ua
§vladyslav.libov@gmail.com

degeneracy of states with increasing mass that can be counted directly, the prefactor $f(m)$ reflects dynamics encoded in Regge trajectories given that $f(m) = \alpha'(m)$, where $\alpha'(m)$ is the slope of the trajectory.

The low-mass, $m < 1.8$ GeV spectra do not exhibit any surprise by following Hagedorn's exponential. The only open questions are the value of the Hagedorn temperature T_H and possible differences between the spectra for various particles. The spectra beyond $m = 1.8$ GeV are different: On the experimental side, the high-mass resonances tend to gradually disappear, their status becoming uncertain. An update of the Hagedorn mass spectrum can be found in Refs. [2–5]. Different Hagedorn temperatures for mesons and baryons from experimental mass spectra, compound hadrons, and combinatorial saturation were studied in Ref. [2].

In any case, the most important issue is the existence of a "melting point," where the resonances are transformed to a continuum of a boiling soup of quarks and gluons. This critical region or point is studied by various methods: statistics and thermodynamics, quantum chromodynamics, lattice QCD calculations, the Massachusetts Institute of Technology (MIT) bag models, Regge poles, and relations derived within analytic S-matrix theory. The research objectives are the order of the assumed phase transition or crossover transition, fluctuations and correlations of conserved charges, and the Fourier coefficients of net-baryon density. For a recent treatment of these issues, see Ref. [15].

In the present paper, we extend the existing panorama by appending the dynamics arising from the behavior of Regge trajectories. Regge trajectories are rich objects containing information on the spectrum of resonances. Although they are usually approximated by infinitely rising linear functions, predicting an infinite number of resonances, in fact, the analytic theory confines the rise of their real part, limiting the number of resonances in nature. Below we show how the nonlinear complex trajectories affect the Hagedorn spectrum.

More details on the Hagedorn spectrum, Hagedorn temperature, and hot phases of hadronic matter can be found in the writings of Johann Rafelski [16–18].

The paper is organized as follows. In Subsec. II A, we discuss various approaches to the density of hadron states, including the Hagedorn model. In Subsec. II B, we discuss complex, nonlinear Regge trajectories and their relation to Hagedorn's density of states. Both the density of states and the hadron spectrum are finite and interrelated, as shown in Subsec. II C by a relevant explicit example. In Sec. III, we discuss the relation between the spectra and the statistical properties of the nuclear matter with possible equations of state of hadronic matter.

II. MELTING HADRONS

The spectrum of resonances and their statistical properties are interrelated. In this section, we study the relation between the mass density of hadronic states given by the Hagedorn spectrum and the dynamics emerging from Regge pole models, inspecting nonlinear Regge trajectories.

In spite of the huge number of papers, the subject remains a topical problem of hadron dynamics with numerous open questions. In this paper, we address the following issues:

(1) the behavior of the meson mass spectrum in the high-mass region;
(2) the roles of the critical temperature and the prefactor in $\rho(m)$ in the Hagedorn model of hadronic spectra; and
(3) the finiteness of the Hagedorn spectrum and its consequences.

A. Density of states (Hagedorn distribution) and resonance spectra (Regge trajectories)

The idea of the spectral description of a strongly interacting gas was suggested by Belenky and Landau [19]. This approach treats resonances on equal footing with stable hadrons. The expression for pressure in this thermodynamic approach in the Boltzmann approximation is given by

$$p = \sum_i g_i p(m_i) = \int_{M_1}^{M_2} dm\, \rho(m)\, p(m), \tag{2}$$

with

$$p(m) = \frac{T^2 m^2}{2\pi^2} K_2\left(\frac{m}{T}\right),$$

where M_1 and M_2 are the masses of the lightest and heaviest hadrons, respectively, and g_i-s are particle degenerations.

It was suggested in Refs. [20–22] that for fixed isospin and hypercharge a cubic density of states, $\rho(m) \sim m^3$, fits the data. Moreover, as argued in Ref. [20], the cubic spectrum can be related to collinear Regge trajectories. Indeed, following the arguments of Burakovsky [23], on a linear trajectory with negative intercept, $\alpha(t) = \alpha' t - 1$, some integer values of $\alpha(t) = J$ correspond to states with negative spin, $J = \alpha(t_J)$, with squared masses $m^2(J) = t_J$. Since a spin-J state has multiplicity $2J + 1$, the total number of states with spin $0 \leqslant J \leqslant j$ at $t = m(j)^2$ is given by

$$N(j) = \sum_{J=0}^{j} (2J + 1) = (j + 1)^2 = \alpha'^2 m^4(j). \tag{3}$$

Hence, the density of states per unit mass interval is obtained as the derivative of this cumulative quantity,

$$\rho(m) = \frac{dN(m)}{dm} = 4\alpha'^2 m^3, \tag{4}$$

and it grows as the cubic power of the mass. Consequently, for a finite number of collinear trajectories, N, the corresponding mass spectrum is given as

$$\rho(m) = 4N\alpha'^2 m^3. \tag{5}$$

A different view on the spectra was advocated by Shuryak [21], who suggested using a quadratic parametrization, completely different from the conventional form:

$$\rho(m) \sim m^2.$$

In both the statistical bootstrap model [1] and in the dual resonance model [24,25] the resonance spectrum takes the form of Eq. (1). In the dual resonance model, $f(m) \sim$

$\frac{d}{dm}\mathrm{Re}\alpha(m^2)$. In this work, we use nonlinear complex Regge trajectories to determine this prefactor, as discussed in the next subsections.

The meson and baryon spectra differ, in particular by their slopes, as shown, e.g., in Refs. [2,3]. More important is the question of the asymptotic behavior of $\rho(m)$ for large masses. In theory, Hagedorn's exponential may rise indefinitely; however, starting from $m \approx 2.5$ GeV resonances are not observed. The question arises of whether it is a "technical" issue (the resonances gradually fade becoming too wide to be detected) or there is a critical point where they melt to a continuum, transforming the hadron matter to a "boiling soup." Remarkably, this point can be illuminated by means of Regge trajectories, as we shall demonstrate in the following.

In the present paper, we concentrate on the meson spectrum, more specifically that of ρ and its excitations. This familiar trajectory is chosen just as a representative example. Other trajectories, including baryonic ones as well as those with heavy (c and b) flavors, will be studied later. We are interested in the high-mass behavior, starting from $m \approx 1.8$ GeV. Beyond this value, the exponential behavior of the Hagedorn spectrum is expected to change drastically. Referring to perfect low- and intermediate-mass fits of Ref. [3], we concentrate now on its behavior above 1.8 GeV.

Note that instead of comparing the density of states $\rho(m)$ to the data it is customary to accumulate states of masses lower than m,

$$N_{\mathrm{exp}} = \sum_i g_i \Theta(m - m_i), \tag{6}$$

where g_i is the degeneracy of the ith state with mass m_i in spin J and isotopical spin I, i.e.,

$$g_i = \begin{cases} (2J_i+1)(2I_i+1), & \text{for nonstrange mesons} \\ 4(2J_i+1), & \text{for strange mesons} \\ 2(2J_i+1)(2I_i+1), & \text{for baryons} \end{cases}.$$

The theoretical equivalent of Eq. (6) is

$$N_{theor}(m) = \int_{m_\pi}^{m} \rho(m')dm', \tag{7}$$

where the lower integration limit is given by the mass of the pion. We identify $f(m)$ in $\rho(m)$ with the slope of the relevant nonlinear complex Regge trajectory $\alpha'(m)$. In the next subsection, we discuss the properties of these trajectories following from the analytic S-matrix theory and duality and present an explicit example of such a trajectory.

B. Regge trajectories

At low and intermediate masses, light hadrons fit linear Regge trajectories with a universal slope, $\alpha' \approx 0.85\ \mathrm{GeV}^2$. As masses increase, the spectrum changes: Resonances tend to disappear. The origin and details of this change are disputable.

Termination of resonances associated with a "ionization point" was also studied in a different class of dual models, based on logarithmic trajectories [26].

Possible links between the Hagedorn spectra and Regge trajectories appear in the statistical bootstrap and dual models

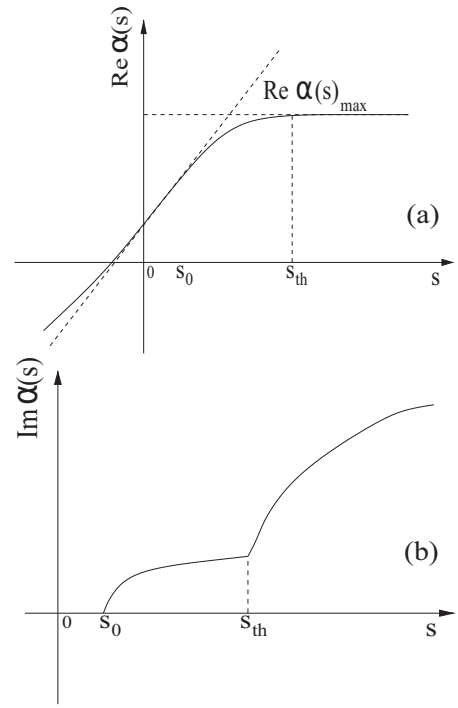

FIG. 1. Typical behavior of the real (a) and imaginary (b) parts of Regge trajectories in dual models with Mandelstam analyticity [14].

[25], according to which the prefactor $f(m)$ in Eq. (1) depends on the slope of the relevant Regge trajectory, $\alpha'(m^2)$, which is a constant for linear Regge trajectories.

We extend the Hagedorn model by introducing the slope of relevant nonlinear Regge trajectories. Anticipating a detailed quantitative analysis, one may observe immediately that a flattening of $\mathrm{Re}\alpha(s = m^2)$,[1] shown in Fig. 1, results in a decrease of the relevant slope $\alpha'(m)$ and a corresponding change in the Hagedorn spectrum. Following Eq. (1), we parametrize

$$\rho(m) = \left(\frac{d}{dm}\mathrm{Re}\alpha(m^2)\right) \times \exp(m/T_H). \tag{8}$$

Based on the decreasing factor $\mathrm{Re}\alpha'$ in Eq. (8), the exponential rise of the density of states slows down near to the melting point around $m \approx 2$–2.5 GeV. The cumulative spectrum, Eqs. (6) and (7), accordingly tends to a constant value.

Any Regge trajectory should satisfy the followings (for a comprehensive review see Ref. [27]):

(1) threshold behavior imposed by unitarity;
(2) asymptotic constraints: the rise of real part of Regge trajectories is limited, $\mathrm{Re}\alpha(s) \leqslant \gamma\sqrt{t}\ln t, \quad s \to \infty$; and
(3) compatibility with the nearly linear behavior in the resonance region (Chew-Frautschi plot).

The threshold behavior of Regge trajectories is constrained by unitarity. As shown by Barut and Zwanziger [28], t-

[1]We use the (here positive) variables s or t interchangeably with crossing symmetry in mind.

channel unitarity constrains the Regge trajectories near the threshold $t \to t_0$ to the form

$$\mathrm{Im}\alpha(t) \sim (t - t_0)^{\mathrm{Re}\alpha(t_0)+1/2}. \tag{9}$$

Here t_0 is the lightest threshold, e.g., $4m_\pi^2$ for the meson trajectories. Since $\mathrm{Re}\alpha(4m_\pi^2)$ is small, a square-root threshold is a reasonable approximation to the above constraint.

In the resonance region below flattening near $m = \sqrt{s} \lesssim 2.5$ MeV, the meson and baryon trajectories are nearly linear (Chew-Frautschi plot). Fixed-angle scaling behavior of the amplitude constrains the trajectories even more, down to a logarithmic behavior [29].

The combination of the threshold behavior Eq. (9) and the above asymptotic behavior suggested the explicit model [30] of trajectories as a sum of square-root thresholds (see the details in Subsec. II C).

There are several reasons why the nonlinear and complex nature of the Regge trajectories is often ignored, namely (1) the observed spectrum of meson and baryon resonances (Chew-Frautschi plot) seem to confirm their linearity; (2) in the scattering region, $t < 0$, the differential cross section, $d\sigma/dt \sim \exp((2\alpha(t) - 2)\ln s)$ is nearly exponential in t; and (3) dual models, e.g., the Veneziano amplitude, are valid only in the narrow-width approximation, corresponding to linear Regge trajectories (hadronic strings). Deviation from linearity is unavoidable, but its practical realization is not easy. Attempts are known in the literature; see, e.g., Refs. [23,31,32] and references therein.

As a final remark, we comment on a typical feature of dual analytic models, namely the extremely broad resonance approximation, suggested in Ref. [14], by which the unitarization procedure, contrary to the narrow resonance (Veneziano-like) models in Fig. 25 of Ref. [14], move the resonance pole from the real (negative) axis to the physical region of broad resonances, harmless to its basic properties, e.g., polynomial boundedness (for more details, see Ref. [14]). This property is essential for the parametrization of our Regge trajectory $\alpha(t)$. Due to our factor $f(m) = (\mathrm{Re}\alpha(m))$, the spectrum is a "mixture" of narrow and wide resonances, and therefore not purely "Hagedornian" anymore.

C. The ρ trajectory and the Hagedorn spectrum

Trajectories satisfying the above requirements have been studied extensively in the past. A particularly simple and transparent nonlinear trajectory was suggested in Refs. [30,33] and is defined as a sum of square-root thresholds formed by stable particles, allowed by quantum numbers. While the imaginary part of such a trajectory starts to be nonzero by exceeding the lightest threshold and rises indefinitely, its real part terminates at the heaviest threshold (see Fig. 1).

Specifically, Ref. [33] defines trajectories as

$$\alpha(s) = \lambda - \sum_i \gamma_i \sqrt{s_i - s}, \tag{10}$$

where all two-particle stable thresholds are included in the sum. For the ρ-meson trajectory, two meson-meson and four baryon-antibaryon channels are taken into account, as listed in Table I along with corresponding thresholds s_i and weights γ_i. Note that for simplicity the same weight is used for all baryon-antibaryon channels.

TABLE I. Parametrization of the ρ trajectory [33].

Channel	s_i	γ_i
$\pi\pi$	0.078	0.127
$K\overline{K}$	0.976	0.093
$N\overline{N}$	3.52	0.761
$\Lambda\overline{\Sigma}$	5.31	0.761
$\Sigma\overline{\Sigma}$	5.66	0.761
$\Xi\overline{\Xi}$	6.98	0.761

The real and imaginary parts of the trajectory described by Eq. (10) with parameters from Table I are shown in Fig. 2. The vertical lines indicate thresholds s_i. As expected, above the highest threshold ($s_6 = 6.98\ \mathrm{GeV}^2$) the real part reduces to a constant, $\mathrm{Re}\alpha = \lambda$.

Putting $s = m^2$ and differentiating the real part of the trajectory with respect to m, we obtain

$$\frac{d}{dm}\mathrm{Re}\alpha(m^2) = \sum_i \frac{\gamma_i m}{\sqrt{s_i - m^2}}, \tag{11}$$

where for a given m the sum includes only terms satisfying $m^2 < s_i$. Substitution into (8) yields

$$\rho(m) = \frac{d}{dm}\mathrm{Re}\alpha(m^2)\exp(m/T) = \sum_{i:\, s_i > m^2} \frac{\gamma_i m}{\sqrt{s_i - m^2}} \exp(m/T). \tag{12}$$

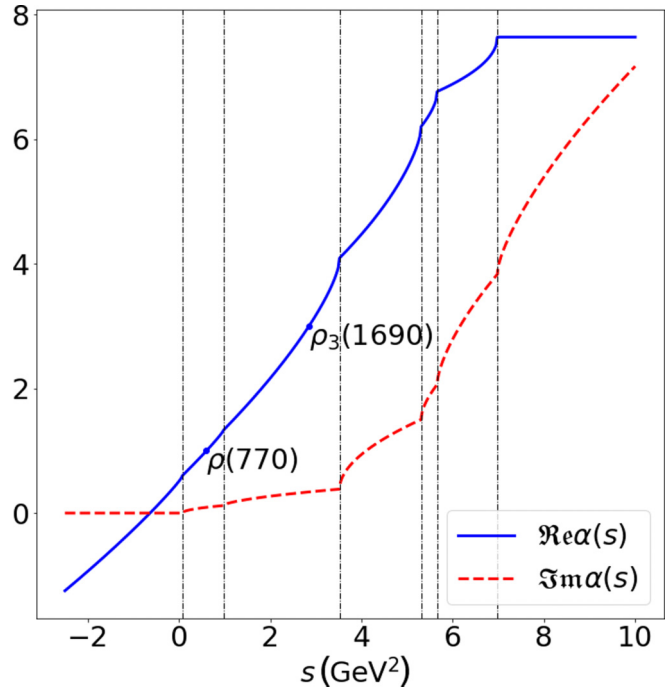

FIG. 2. Real and imaginary parts of the ρ trajectory.

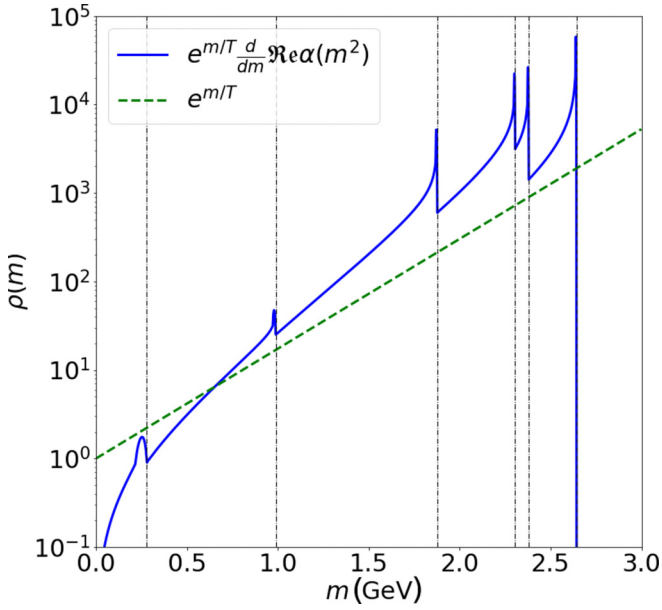

FIG. 3. Mass density $\rho(m)$ calculated by using the derivative of the smoothed ρ-meson trajectory as a prefactor, Eq. (12). The exponential density without any prefactor is also shown (dashed line), using the same temperature and normalization. Above the highest threshold, the derivative, and hence the density vanishes (not seen due to the logarithmic scale).

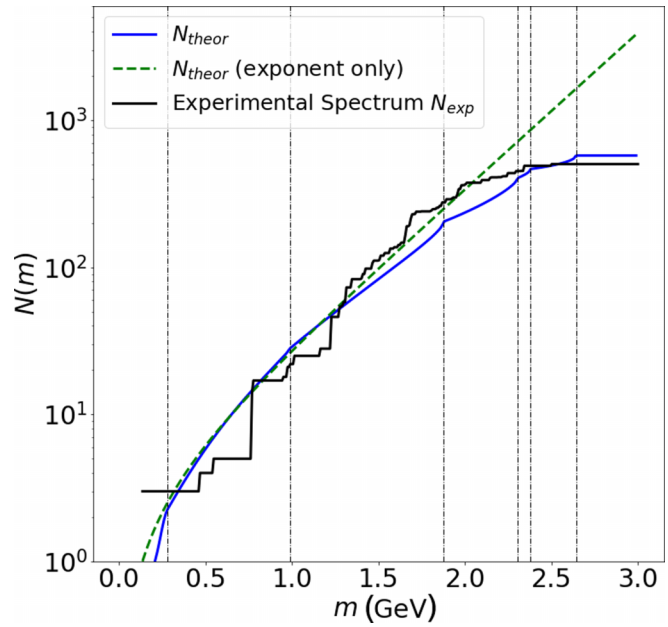

FIG. 4. Hadron mass spectrum $N_{\rm theor}$ from Eq. (7) using the mass density of Eq. (12) (blue line) compared to data (black histogram). Additionally, $N_{\rm theor}$ obtained from a simple exponential mass density is also shown (green dashed line).

As in Eq. (11), the sum includes for a given m only terms with $s_i > m^2$; the derivative and thus the mass density vanish above the highest threshold. At the thresholds s_i, the derivative and hence the density diverge. However, the relevant integral, Eq. (7), stays finite. For simplicity, we smooth the trajectory $\mathrm{Re}\alpha(s)$ in the vicinity of the thresholds using splines. With this procedure, the derivative becomes finite and continuous and can be integrated numerically. An example of the resulting mass density $\rho(m)$ is shown in Fig. 3.

The mass density $\rho(m)$ can now be integrated using Eq. (7) in order to obtain the theoretical prediction for the mass spectrum, $N_{\rm theor}(m)$. Figure 4 shows the result, together with the experimental cumulative spectrum $N_{\rm exp}(m)$ using the states listed by the Particle Data Group [6].

As expected, $N_{\rm theor}(m)$ flattens above the highest threshold (corresponding to $m \approx 2.65$ GeV), since the density $\rho(m)$ defined with Eq. (12) vanishes in that region. This is consistent with the experiment, since no unflavored mesons have been observed above $m \approx 2.5$ GeV [6]. On the other hand, the integrated spectrum using a simple form $\rho = e^{m/T}$ is rising indefinitely, thus failing to describe flattening of the data at high masses.

The temperature and normalization used in Fig. 4 were determined from a least-squares fit to data. The fit was performed separately for two models (a simple exponent and an exponent with a prefactor). The optimal temperature for the pure exponent is $T = 0.41$ GeV, slightly larger but generally consistent with the previous studies. Inclusion of the prefactor steepens the curve (see, e.g., Fig. 3), and thus a larger temperature ($T = 1.45$ GeV) is required to fit the data.

Resonances may melt for two reasons: (1) for square-root $\alpha(s)$ trajectories (10), whose real part terminates at some large mass and consequently the derivative vanishes, or (2) for densities of resonances modelled by powerlike functions rather than exponentials.

The above is only a representative example intended to show the interrelation between the Hagedorn spectrum and the one based on nonlinear complex Regge trajectories (Chew-Frautchi plot). The present results can be extended in several directions:

(1) by including other trajectories, mesonic and/or baryonic;
(2) by including heavy flavors such as b quarks, both in the Hagedorn and Regge spectra; and
(3) working with alternative parametrizations of nonlinear, complex Regge trajectories.

III. BOILING QUARKS AND GLUONS

In the previous section, we inspected the spectrum of resonances by combining two different approaches: statistical (Hagedorn) and dynamical (Regge). We have focused on the region of heaviest resonances, the region where hadrons may melt transforming in a boiling "soup" of quarks and gluons. Melting may happen in different ways, characterized by the details for a phase transition of colorless hadronic states into a quark-gluon soup, whatever it be [34]. In terms of hadron strings, this process corresponds to breakdown (fragmentation) of a string. Lacking any theory of confinement providing a quantitative description of interacting string, we will not pursue this model. Instead we use thermodynamics adequate in this situation. To complement the previous section, we

present our arguments below related to the possible change of phase from a different, thermodynamic perspective.

The Hagedorn exponential spectrum of resonances Eq. (1) results in a singularity in the thermodynamic functions at critical temperature $T = T_c$ and in an infinite number of effective degrees of freedom in the hadronic phase. Also, as shown in Ref. [35], a Hagedorn-like mass spectrum is incompatible with the existence of the quark-gluon phase. To form a quark phase from the hadronic phase, the hadron spectrum cannot grow more quickly than a power. This is possible [21] in case of a simple power parametrization $\rho \sim m^k$, compatible with $k \approx 3$, for the observable mass spectrum in the interval 0.2–1.5 GeV. Assuming ideal contributions to thermodynamical quantities, we hence take energy density in the form

$$\epsilon = \int_0^\infty \rho(m) T^4 \sigma(m/T) dm = \lambda_k T^{k+5}, \tag{13}$$

and obtain the corresponding pressure and sound velocity square as follows:[2]

$$p = \frac{\lambda_k}{k+4} T^{k+5}, \quad c_s^2 = 1/(k+4). \tag{14}$$

The above empirical power-like behavior has also theoretical background. In Ref. [36], an asymptotic, $T \gg m$, EOS was derived by using the S-matrix formulation of statistical mechanics [37]. It was shown that the existence of the forward cone in hadronic interactions with nondecreasing total cross sections, i.e., pomeron dominance, confirmed by numerous experiments at high energies, results in an asymptotic, $T \gg m$ EOS $p(T) \sim T^6$ where m is a characteristic hadron (e.g., pion) mass. The inclusion of nonasymptotic (secondary) Regge terms produces a minimum in the $p(T)$ dependence at negative pressure, with far-reaching observable consequences.

Such an asymptotic formula for the pressure, different from the standard $p(T) \sim T^4$, was derived on different grounds also in Ref. [21].

The unorthodox $p \sim T^6$ asymptotic behavior is orthogonal to the canonical (perturbative QCD) form $\sim T^4$. Still, it cannot be rejected, e.g., when assuming a screening of the action of large-distance van der Waals forces at high temperatures and densities.

In Ref. [38], the asymptotic form $\sim T^6$ was extended to lower temperatures by adding nonasymptotic Regge-pole exchanges. The resulting EOS is

$$p(T) = aT^4 - bT^5 + cT^6, \tag{15}$$

where a, b, c are parameters connected with Regge-pole fits to high-energy hadron scattering. The remarkable property of this EOS, apart from the nonstandard asymptotic behavior, $\sim T^6$, is the appearance of the nonasymptotic term T^5 with negative sign, creating a local minimum with negative pressure. This metastable state with negative pressure was shown [39] to produce inflation of the universe.

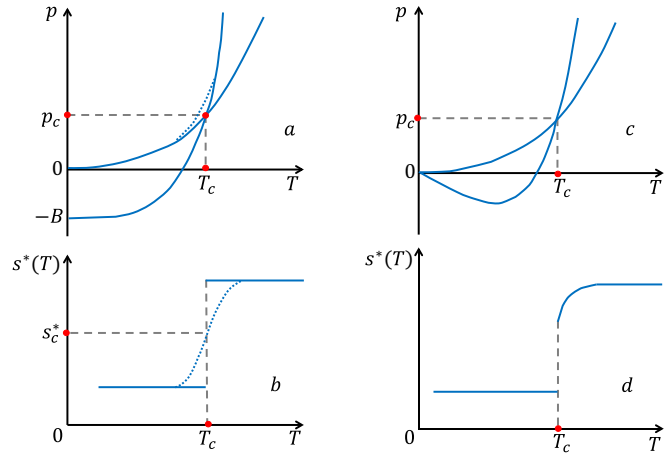

FIG. 5. Icons a and b show the standard bag EoS, Eq. (17), with constant B; here $s^*(T) = s(T)/T^3$. The dotted line corresponds to the modified bag EoS (23). Icons c and d feature the Källmann EoS [41], where $B = AT$.

In the next part, we discuss the phase transition of colorless hadronic states into quark-gluon soup in the framework of modified quark bag models.

The standard bag equation of state assuming, for simplicity, vanishing chemical potential, $\mu = 0$:

$$p_q(T) = \frac{\pi^2}{90} \nu_q T^4 - B, \tag{16}$$

$$p_h(T) = \frac{\pi^2}{90} \nu_h T^4, \tag{17}$$

where $p_q(T)$ and $p_h(T)$ are pressure in the quark-gluon plasma (QGP) and in the hadronic gas phase, respectively, B is the bag constant, and $\nu_{q(h)}$ is the number of degrees of freedom in the QGP (hadronic gas). From Eqs. (16) and (17), one finds the characteristic parameters of the phase transition [see Fig. 5(a)]:

$$p_c = B\nu_h/(\nu_q - \nu_h), \quad T_c = [90B/\pi^2(\nu_q - \nu_h)]^{1/4}. \tag{18}$$

Since $s(T) = dp(T)/dT$, the relevant formula for the entropy density can be rewritten as [see Fig. 5(b)]

$$s(T) = (2\pi^2 T^3/45)\nu_h[1 - \Theta(T - T_c) + \nu_q \Theta(T - T_c), \tag{19}$$

$$s^*(T) = s(T)/T^3, \quad s_c^* = s_c/T_c^3, \quad s_c = \frac{\pi^2 T_c^3}{45}(\nu_h + \nu_q). \tag{20}$$

The above simple bag model EOS can also be modified [41,42] by making the bag "constant" T dependent, $B(T) = AT$, to produce a metastable QGP state with negative temperature [see Figs. 5(c) and 5(d)]:

$$p_q(T) = (\pi^2/90)\nu_q T^4 - AT, \quad p_h(T) = (\pi^2/90)\nu_h T^4. \tag{21}$$

[2]Note that the definition of entropy density s, energy density ϵ, and velocity of sound c_s in the case of $\mu = 0$:

$$s(T) = p'(T), \ \epsilon(T) = Ts - p, \ \ c_s^2 = \frac{dp}{d\epsilon} = \frac{p'}{Tp''} = \frac{s}{Ts'}.$$

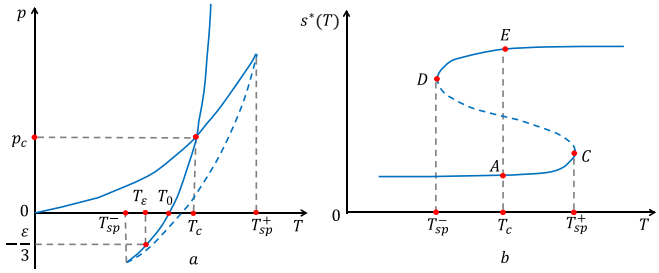

FIG. 6. Modified bag EOS Eq. (24), including metastable states. Icon *a* is the $p(T)$ dependence while icon *b* is $s^*(T) = s(T)/T^3$.

In Ref. [40], EOS Eq. (19) was modified by the replacement

$$\Theta(T - T_c) \to \frac{1}{2}\left[1 + \tanh\left(\frac{T - T_c}{\Delta T}\right)\right], \tag{22}$$

where ΔT is a parameter related to the smoothness of a crossover transition. With the above substitution, the EOS can be rewritten as

$$\frac{T - T_c}{\Delta T} = \operatorname{arctanh}(\Gamma \Delta s^*), \tag{23}$$

where $\Gamma = 45/[\pi^2(\nu_q - \nu_h)]$, $\Delta s^* = s^* - s_c^*$, behaving as shown by the dotted line in Fig. 5(b). This modification, however, smoothes down first-order phase transitions in EOS, thus excluding possible metastable states. It may serve as a springboard for a further modification suggested in Ref. [43], namely:

$$(T - T_c)/\Delta T = \operatorname{arctanh}(\Gamma \Delta s^*) - \gamma \Delta s^*, \tag{24}$$

where γ is the "metastability parameter." For $\Gamma - \gamma > 0$, EOS Eq. (24) is of the same type as Eq. (23), while for $\Gamma - \gamma < 0$ a loop emerges in the entropy density [Fig. 6(b)], similar to the loop in the density to pressure dependence, described by the van der Waals equation or the EOS of a magnet in vicinity of the Curie point, replacing Δs^* with the order parameter of the phase transition and substituting $(T - T_c)/\Delta T$ by the corresponding conjugate field. For $\Gamma - \gamma < 0$, the curve $s^*(T)$ contains a nonphysical region (interval CD) with $ds/dT < 0$. The intervals (AC) and (DE) of $s^*(T)$ correspond to metastable states, C and D being the spinodal points where $ds/dT \sim c_s^{-2}$, with c_s being the sound speed.

Another important feature of the EOS Eq. (24) is that for $\Gamma - \gamma = 0$ it describes second-order phase transitions, with singular behavior of the thermal capacity at $T = T_c$. Really, in this case, we have $T - T_c \sim (\Delta s^*)^3$ near $T = T_c$.

IV. SUMMARY AND CONCLUSIONS

We related two different approaches to the critical point in the hadron spectra using statistical (Hagedorn) and dynamical (Regge) models. Our innovation is in the use of nonlinear Regge trajectories, predicting a limited spectrum of hadron states, ignored in most of the papers on Regge-pole theory. Although our analyses is limited to the simple case of the ρ meson spectrum, this technique and the results can (and will) be extended to other hadrons.

In this work, we showed that the observed saturation of the number of hadrons as a function of mass can be easily explained in the Regge theory by using nonlinear trajectories and attributing the prefactor in Hagedorn's density to the slope of the corresponding Regge trajectory. Due to flattening of the latter, the slope vanishes, and the number of states flattens. In this way, we enter the most intriguing of the strong interaction, namely the expected transition of excited colorless hadrons into the hypothetical boiling soup of quarks and gluons.

Flattening of the exponential density of states and of the linear rise of Regge trajectories point to the same phenomenon, namely quark deconfinement ("melting" of hadrons). The two phenomena are correlated but they are not identical. Their combined study and further fits to the data may reduce the available freedom of the relevant parametrizations and tell us more about the onset of deconfinement.

The maximum mass of existing resonances depends on the parameters fitted to the observed resonances. Resonances tend to disappear (fade) beyond some mass. Their nonobservability may have two reasons: Either they are not visible because of their large width (decay time) or they melt, losing their individual features. These phenomena, especially the second, "boiling" phase, can be studied also in the framework of thermodynamics, e.g., by studying the relevant equation of state (EoS).

ACKNOWLEDGMENTS

We thank Wojciech Broniowski for useful correspondence on the subject of this paper. L.J. was supported by the National Academy of Sciences of Ukraine's Grant No. 1230/22-1 "Fundamental properties of matter" and by the NKFIH Grant No. K133046; T.B. acknowledges support from the Hungarian National Office for Research, Development and Innovation, NKFIH under the Project No. K123815; I.S. was supported the by the NKFIH Grant No. K133046 and by the ÚNKP-22-3 New National Excellence Program of the Ministry for Innovation and Technology from the source of the National Research, Development and Innovation Fund.

[1] R. Hagedorn, Nuovo Cimento Suppl. **3**, 147 (1965).
[2] W. Broniowski and W. Florkowski, Phys. Lett. B **490**, 223 (2000).
[3] W. Broniowski, W. Florkowski, and L. Y. Glozman, Phys. Rev. D **70**, 117503 (2004).
[4] T. D. Cohen and V. Krejcirik, J. Phys. G: Nucl. Part. Phys. **39**, 055001 (2012).
[5] J. Cleymans and D. Worku, Mod. Phys. Lett. A **26**, 1197 (2011).
[6] R. L. Workman, V. D. Burkert, V. Crede, E. Klempt, U. Thoma, L. Tiator, K. Agashe, G. Aielli, B. C. Allanach, C. Amsler *et al.* (Particle Data Group), Prog. Theor. Exp. Phys. **2022**, 083C01 (2022).
[7] F. Bigazzi, T. Canneti, and A. L. Cotrone, J. High Energ. Phys. 01 (2023) 034.
[8] B. Bringoltz and M. Teper, Phys. Rev. D **73**, 014517 (2006).

[9] M. Caselle, A. Nada, and M. Panero, J. High Energy Phys. 07 (2015) 143; **11**, 016(E) (2017).
[10] D. Kutasov and N. Seiberg, Nucl. Phys. B **358**, 600 (1991).
[11] K. Huang and S. Weinberg, Phys. Rev. Lett. **25**, 895 (1970).
[12] S. H. H. Tye, Phys. Lett. B **158**, 388 (1985).
[13] J. J. Atick and E. Witten, Nucl. Phys. B **310**, 291 (1988).
[14] A. I. Bugrij, G. Cohen-Tannoudji, L. L. Jenkovszky, and N. A. Kobylinsky, Fortschr. Phys. **21**, 427 (1973).
[15] V. Vovchenko, M. I. Gorenstein, C. Greiner, and H. Stoecker, Phys. Rev. C **99**, 045204 (2019); V. Vovchenko, M. I. Gorenstein, C. Greiner, and H. Stoecker, arXiv:1911.06420.
[16] J. Rafelski, Eur. Phys. J. A **51**, 114 (2015).
[17] M. Hadrons, in *Boiling Quarks - From Hagedorn Temperature to Ultra-Relativistic Heavy-Ion Collisions at CERN With a Tribute to Rolf Hagedorn*, 1st ed., edited by J. Rafelski (Springer, Berlin, 2016).
[18] T. Ericson and J. Rafelski, CERN Courier, Sept. 4, 2003.
[19] S. Z. Belenky and L. D. Landau, Sov. Phys. Uspekhi **56**, 209 (1955); Nuovo Cimento **3**, 15 (1956).
[20] E. V. Shuryak, Sov. J. Nucl. Phys. **16**, 220 (1973).
[21] E. V. Shuryak, Phys. Rep. **61**, 71 (1980); E. V. Shuryak, *The QCD Vacuum, Hadrons, and the Superdense Matter* (World Scientific, Singapore, 1988).
[22] L. Burakovsky and L. P. Horowitz, Nucl. Phys. A **614**, 373 (1997).
[23] L. Burakovsky, arXiv:hep-ph/9805286.
[24] S. Fubini and G. Veneziano, Nuovo Cimento A **64**, 811 (1969).
[25] S. Frautschi, Phys. Rev. D **3**, 2821 (1971); W. Nahm, Nucl. Phys. B **45**, 525 (1972).
[26] D. D. Coon, Phys. Lett. B **29**, 669 (1969); M. Baker and D. D. Coon, Phys. Rev. D **2**, 2349 (1970).
[27] A. A. Trushevsky, Ukr. J. Phys. **66**, 97 (2021).
[28] A. O. Barut and D. E. Zwanziger, Phys. Rev. **127**, 974 (1962).
[29] A. I. Bugrij, Z. E. Chikovani, and L. L. Jenkovszky, Z. Phys. C: Part. Fields **4**, 45 (1980).
[30] A. I. Bugrij and N. A. Kobylinskij, Ann. Phys. **487**, 297 (1975).
[31] R. Fiore, L. L. Jenkovszky, V. Magas, F. Paccanoni, and A. Papa, Eur. Phys. J. A **10**, 217 (2001).
[32] R. Fiore, L. L. Jenkovszky, F. Paccanoni, and A. Prokudin, Phys. Rev. D **70**, 054003 (2004).
[33] A. I. Bugrij and N. A. Kobylinskij, Preprint ITP-75-50E, Kiev, 1975.
[34] T. S. Biró, A. Jakovác, and Z. Schramm, Eur. Phys. J. A **53**, 52 (2017).
[35] G. N. Fowler and R. M. Weiner, Phys. Lett. B **89**, 394 (1980).
[36] L. L. Jenkovszky and A. A. Trushevski, Nuovo Cimento A **34**, 369 (1976).
[37] R. Dashen, S. Ma, and H. J. Bernstein, Phys. Rev. **187**, 345 (1969).
[38] A. I. Bugrij and A. A. Trushevsky, JETP **73**, 3 (1977).
[39] A. I. Bugrij and A. A. Trushevsky, Astrofizika **13**, 177 (1977).
[40] J. P. Blaizot and J.-Y. Ollitrault, Phys. Lett. B **191**, 21 (1987).
[41] C.-G. Källman, Phys. Lett. B **134**, 363 (1984).
[42] V. G. Boiko, L. L. Jenkovszky, and V. M. Sysoev, Sov. J. Part. Nucl. **22**, 326 (1991).
[43] V. G. Boyko, L. L. Jenkovszky, and V. M. Sysoev, Z. Phys. C - Part. Fields **45**, 607 (1990).